

## Current-controlled bi-stable domain configurations in $\text{Ni}_{81}\text{Fe}_{19}$ elements: An approach to magnetic memory devices

H. Koo, C. Krafft, and R. D. Gomez<sup>a)</sup>

*Department of Electrical and Computer Engineering, University of Maryland, College Park, Maryland 20742 and Laboratory for Physical Sciences, 8050 Greenmead Drive, College Park, Maryland 20740*

(Received 26 February 2002; accepted for publication 24 May 2002)

The discovery of current-switchable bi-stable remanent domain configurations on small ferromagnetic islands is reported. Rectangular NiFe islands with a thickness of 50 to 100 nm and lateral dimensions on the order of several microns were imaged using magnetic force microscopy after application of 10 ns current pulses through the material. The closure configuration can be set into either the 4 or 7 domain configuration by applying positive or negative current polarity at density on the order  $10^7$  A/cm<sup>2</sup>. The chirality of the closure patterns is fixed, implying that only two rather than four states are stable in these patterns. The possibility of using these configurations as a means of storing a logic state for memory applications is discussed. © 2002 American Institute of Physics. [DOI: 10.1063/1.1495883]

The general method to assign a “1” or “0” in solid state magnetic memory devices is to orient the remanent magnetization of ferromagnetic elements in one of two opposite directions. Thus, the magnetic properties of small particles as well as new ways to switch the magnetization other than by applying an external magnetic field are topics of intense research activity.<sup>1–4</sup> In this letter, we offer an alternative approach to storing and reading binary information in magnetic systems. Specifically, we introduce the idea that a bi-stable remanent domain configuration of a ferromagnetic island, which is selectable by a current pulse through the material, can be a simple and viable option for magnetic random access memory applications.

In a previous investigation, we established that in small rectangular NiFe thin film islands, the number of possible configurations at remanence ( $H_{\text{applied}}=0$ ) is finite.<sup>5</sup> In the case where the length-to-width ratio (referred to as the aspect ratio) is between 1 and 4, and for thickness  $\sim 100$  nm thin or less, the remanent states are predominantly 4- or 7-domain configurations. The four-domain (4D) structure is comprised of four  $90^\circ$  walls emanating from the corners and one  $180^\circ$  Néel wall at the center and parallel to the shape-induced easy axis. The seven-domain (7D) configuration, on the other hand, contains four  $90^\circ$  walls as in the previous case, but the  $180^\circ$  wall is replaced by a diamond-shaped domain at the center of the island, with an internal magnetization along the hard axis. These two states represent local minima of the energy and are determined by competition between the reduction of the magnetostatic energy and the cost of forming domain walls. From numerical calculations, the 7D configuration is about 25% lower in magnetostatic energy. We discovered that reversible 7D-4D state selection can be achieved by driving current pulses through the element in a process that involves domain wall displacement,<sup>6</sup> and submit that these two distinct domain configurations can be used to encode binary information.

We patterned 100-nm-thick permalloy films on silicon with native oxide into  $8.3 \mu\text{m} \times 17 \mu\text{m}$  islands using conventional lift-off techniques. Gold pads were subsequently patterned as electrical contacts at both ends of the islands to enable current flow along the long axis. Figure 1(a) shows the geometry of the patterns. The magnetic images were obtained by magnetic force microscopy. Single-shot 10 ns current pulses were applied, generated using capacitive discharge, through the material. The 7D configuration [Fig. 1(b)] was observed prior to application of any external

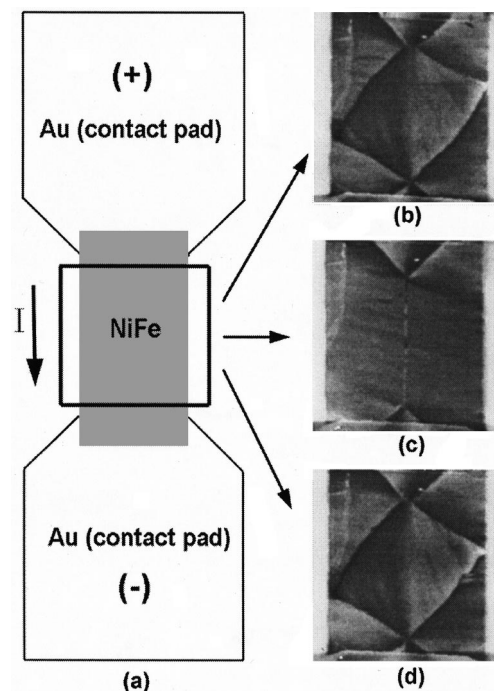


FIG. 1. Bi-stable domain configurations of  $8.3 \mu\text{m} \times 17 \mu\text{m} \times 100$  nm NiFe pattern. (a) Schematic diagram of pattern with contact pads and magnetic force microscopy image (b) of the as-prepared, 7D closure, (c) after current application of a 10 ns pulse with density  $-4.25 \times 10^7$  A/cm<sup>2</sup>, forming a 4D closure, and (d) after current application of a 10 ns pulse of density  $+3.65 \times 10^7$  A/cm<sup>2</sup>.

<sup>a)</sup> Author to whom correspondence should be addressed; electronic mail: rdgomez@eng.umd.edu

stimuli. The central domain is entirely visible, along with portions of the top and bottom domains. A small part of the contact pad is also present at the bottom. This state changed into the 4D configuration shown in Fig. 1(c) after applying a *single* pulse of current density  $-4.25 \times 10^{11}$  A/m<sup>2</sup> for 10 ns. The transition is reversible and the 7D configuration in Fig. 1(d) can be recovered from the four-domain structure by applying a single current pulse of density  $+3.65 \times 10^{11}$  A/m<sup>2</sup>. Note that Figs. 1(b) and 1(d) are essentially identical including the chirality of the closure structures. We performed many experiments on several islands from which we draw the following general characteristics:

- (1) A critical current density is required to change state, below which no reorientation can be achieved regardless of the number of pulses applied.
- (2) Once reoriented, succeeding current pulses of the same polarity and magnitude cause no further effects.
- (3) The critical current density is nearly the same for all islands of similar geometry, but increases with aspect ratio.
- (4) There are only two states observed, with specific chirality of the closure pattern.
- (5) Single pulse selectable (SPS) configurations were observed only for an aspect ratio below 2.7. Since our patterns had a uniform length of 17  $\mu\text{m}$ , the narrowest islands that showed SPS was 6.3  $\mu\text{m}$ . Islands that had larger aspect ratios showed domain wall displacement after the pulses and some eventually underwent reconfiguration. The transition, however, was not predictable.
- (6) Lower thicknesses ( $<45$  nm) produced complex multi-domain states for all the geometries used in this experiment.
- (7) The configuration can be cycled (indefinitely) without variation in the current densities.

In the absence of high-speed imaging, it is impossible to ascertain the exact dynamics of the reconfiguration. However, we offer an explanation on the basis of domain drag theories developed by Berger and Hung more than a decade ago.<sup>7-9</sup> By considering the motion of the electrons as well as the assumption of the structure of the domain wall, it is found that the force can be cast in the form,<sup>10</sup>

$$F_x \propto -v_x^2 \frac{d}{dx} \left( \frac{d\theta}{dx} \right)^2, \quad (1)$$

where  $v_x$  is the speed of the conduction electron and  $\theta(x)$  is the variation of the angle between the individual moments comprising a domain wall. In the case of 180° Néel wall, the angular profile is given as

$$\theta = \pi - 2 \tan^{-1}(e^{-\pi x/\delta}), \quad (2)$$

where  $\delta$  is the domain wall width. We point out this model for the angular variation is an odd function with respect to the center of the wall, i.e.,  $x=0$ , so that  $d(d\theta/dx)^2/dx$  has an opposite sign on each side of the wall. Thus, integration of the total force on the wall vanishes when the electron density is assumed constant or in the case of zero current flow. However when current flows, the density of conduction states between the sides of the wall are not the same, i.e.,  $\rho(E_F + eV) > \rho(E_F)$ , where  $V$  is the voltage drop between

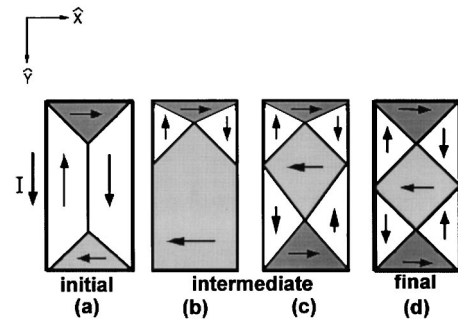


FIG. 2. Schematic diagram of the dynamics of domain wall motion for the 4D to 7D transition.

the walls. Hence, a non-zero net force exists on the wall in the direction of electron flow or opposite the direction of the current. The salient conclusion from this analysis is that a force perpendicular to a wall exists when a polarized electron current traverses a domain wall. The force is directed along the electron velocity or opposite the direction of current flow.

Apart from  $s-d$  exchange, there is the interaction between the current induced magnetic field and the local magnetization. Indeed, the switching of layers in giant magnetoresistance devices in the current-perpendicular-to-the-plane arrangement is attributed to this interaction.<sup>10</sup> In our experiments, the maximum field inside the films can be estimated by using Ampere's law to be  $Jr/2 \approx (10^{11} \text{ A/m}^2)(10^{-7} \text{ m}) = 10^4 \text{ A/m} = 126 \text{ Oe}$ . While the magnitude is above the wall coercivity, this field cannot induce a net wall translation since it is rotational. For instance, the direction of the field on the top is opposite the bottom surface, which would result in a distortion rather than a translation of the wall. Other mechanisms such as hydromagnetic force may contribute as well but the thickness of our films is low enough that  $s-d$  exchange is believed to be the dominant force.<sup>6</sup>

Keeping this in mind, we offer the following schematic diagram of the domain wall motion that may explain the observed effect. For clarity, we first explain the 4D to 7D transition, despite the experimental observation that the initial transition is from the 7D to 4D domain state. During the application of the (positive) pulse in the direction shown in Fig. 2, the 90° walls experience an upward force. The intermediate state during the pulse is then expected to be similar to Fig. 2(b), where the bottom domain expands at the expense of the other (upper) domains. However, since the magnetostatic energy increases with domain size, it is energetically favorable for the bottom domain to breakup via the formation of a closure structure at the bottom end. This is illustrated in Fig. 2(c). The final configuration [Fig. 2(d)] is formed as the system relaxes to ensure that the domains are commensurate with the 90° wall boundaries. We point out that once the 7-D configuration has been achieved, successive identical pulses do not cause any reconfiguration. The potential barrier to revert back to a 4D configuration is higher when the top and bottom domains are along the same direction. However, the return to the original 4D configuration can be achieved by a current pulse of *negative* polarity with a somewhat higher density. The reverse process is illustrated in Fig. 3. Downward forces act on all walls, causing the central domain to be displaced towards the bottom and eventually annihilate the original closure structure. This

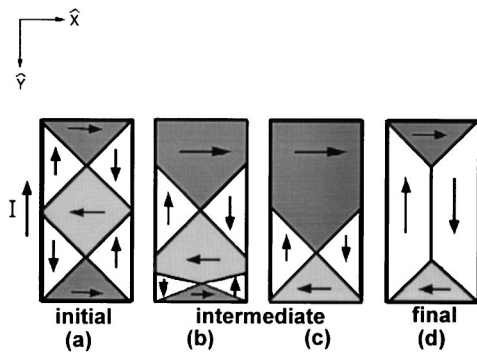


FIG. 3. Schematic diagram of the dynamics of domain wall motion for the 7D to 4D transition.

leaves behind a large upper domain. However, in contrast with the previous case, it does not subdivide into smaller domains. As it is apparently energetically costlier to create domains with  $-x$  magnetization, we suspect that an “anisotropy” favoring the  $+x$  direction is present in the films.

One could argue on the basis of symmetry that the 4D configuration can be similarly achieved by applying a *positive* current pulse. If this were true, then the resulting 4D pattern will have the opposite sense of rotation. This (counterclockwise) chirality, however, was never experimentally observed. This could be explained by assuming as was done earlier, that there is a *unidirectional* anisotropy that breaks the symmetry between  $+x$  and  $-x$  directions. If, for instance, the  $+x$  is favored, this will introduce a predilection for wall motion along the  $+y$  direction (increasing the size of the favorable  $+x$  magnetized domain) but not the other. We do not yet know the exact origin of the unidirectional anisotropy in our case, because there is no obvious source of exchange biasing. This issue is currently under further study.

One possibility might be due to the Amperian fields from the gold contacts. The contacts overlap the ferromagnetic element from above, and highly localized fields on the order of  $\sim 100$  Oe are generated during the pulse in the direction defined by the right hand rule. As the field mainly affects the area directly underneath, slight variations in the degree of overlap in either ends could induce the asymmetry in the transitions. For instance in the case shown in Fig. 2(b) and noting that the overlap is larger at the bottom, the field from a positive pulse favors domains with magnetization  $+x$  to form at the bottom. A negative pulse on the other hand lacks the additional field to induce  $-x$  magnetized domain to form at the top. Hence, the 7D transition using negative pulse is not observed. Similar arguments can be made to explain the features of the 4D to 7D transition. A consequence of this analysis is that in the ideal case of perfect contact alignment at both ends, then the transitions would probably involve a chirality change of the same pattern, rather than a domain reconfiguration.

The other intriguing feature of these elements is that the original configuration can be recovered by applying a second

pulse of the *same* polarity but at substantially larger current density. For example, the 7D configuration can be recovered from a reoriented 4D structure by applying twice the current density of the previous pulse, i.e.,  $8.5 \times 10^{11}$  A/m<sup>2</sup>. Clearly, the aforementioned dynamical model is insufficient to explain the effect, particularly since the model predicts the opposite chirality. The mechanism is probably quite complex, which may involve the reflection of a moving domain wall at the edge with appropriate damping.

Despite our incomplete understanding of the details of the switching, this discovery suggests a potential memory device that can be selectable either by a bipolar or monopolar power source. The storage element is a single island of NiFe. The effect is not only expected to persist but requires less current at smaller lateral dimensions. From our experiments, we have observed 7D and 4D configurations of 25 nm NiFe patterns with dimensions  $250 \text{ nm} \times 125 \text{ nm} \times 25 \text{ nm}$ ,<sup>5</sup> which is instrument limited. Efforts by other researchers on much smaller islands have similarly yielded finite domain configurations that could very well be selectable using current pulses.<sup>11</sup>

Finally, we address the issue of reading the state. The difference between a 4D and 7D pattern is manifested in the reversal of the magnetization of one of the end domains. Thus, one can monitor the magnetization of the end domain by means of a tunnel magnetoresistance by putting an oxide barrier and another spin detecting electrode. A more practical approach is by means of the so-called ballistic nanocontact magnetoresistance<sup>12</sup> and accomplished by placing another spin-polarized electrode in contact with part of the end domain. If the contact area is small enough, the spin polarized electrons from the element would conduct through the constriction without spin flipping. In this case, the transmission probability will be governed predominantly by the relative magnetic alignment of the sensing electrode and the end-domain of the memory element.

This work is supported under NSF Grants ECS-9984797 (CAREER) and ECS-0115327.

<sup>1</sup>J. C. Slonczewski, *J. Magn. Magn. Mater.* **159**, L1 (1996).

<sup>2</sup>E. B. Myers, D. C. Ralph, J. A. Katine, R. N. Louie, and R. A. Buhrman, *Science* **285**, 687 (1999).

<sup>3</sup>J. A. Katine, F. J. Albert, R. A. Buhrman, E. B. Myers, and D. C. Ralph, *Phys. Rev. Lett.* **84**, 3149 (2000).

<sup>4</sup>C.-Y. You and S. D. Bader, *J. Magn. Magn. Mater.* **195**, 488 (1999).

<sup>5</sup>R. D. Gomez, T. V. Luu, A. O. Pak, K. J. Kirk, and J. N. Chapman, *J. Appl. Phys.* **85**, 6163 (1999).

<sup>6</sup>L. Gan, S. H. Chung, K. Aschenbach, M. Dreyer, and R. D. Gomez, *IEEE Trans. Magn.* **36**, 3047 (2000).

<sup>7</sup>L. Berger, *J. Appl. Phys.* **55**, 1954 (1984).

<sup>8</sup>L. Berger, *J. Appl. Phys.* **71**, 2721 (1992).

<sup>9</sup>C. Y. Hung, Ph.D. Thesis, Carnegie Mellon University (1990).

<sup>10</sup>K. Bussman, G. A. Prinz, and S.-F. Cheng, *Appl. Phys. Lett.* **75**, 2476 (1999).

<sup>11</sup>See, for example, R. L. White, *J. Magn. Magn. Mater.* **242–245**, 21 (2002).

<sup>12</sup>N. Garcia, M. Munoz, and Y.-W. Zhao, *Phys. Rev. Lett.* **82**, 2923 (1999).

Applied Physics Letters is copyrighted by the American Institute of Physics (AIP). Redistribution of journal material is subject to the AIP online journal license and/or AIP copyright. For more information, see <http://ojps.aip.org/aplo/aplcr.jsp>  
Copyright of Applied Physics Letters is the property of American Institute of Physics and its content may not be copied or emailed to multiple sites or posted to a listserv without the copyright holder's express written permission. However, users may print, download, or email articles for individual use.